



HAL
open science

Complex Thermo-Mechanical Approaches to Study the Behavior of High-Temperature Alloys

Vincent Bonnand, Didier Pacou

► **To cite this version:**

Vincent Bonnand, Didier Pacou. Complex Thermo-Mechanical Approaches to Study the Behavior of High-Temperature Alloys. Aerospace Lab, 2016, 12, p. 1-12. 10.12762/2016.AL12-04 . hal-01511774

HAL Id: hal-01511774

<https://hal.science/hal-01511774>

Submitted on 21 Apr 2017

HAL is a multi-disciplinary open access archive for the deposit and dissemination of scientific research documents, whether they are published or not. The documents may come from teaching and research institutions in France or abroad, or from public or private research centers.

L'archive ouverte pluridisciplinaire **HAL**, est destinée au dépôt et à la diffusion de documents scientifiques de niveau recherche, publiés ou non, émanant des établissements d'enseignement et de recherche français ou étrangers, des laboratoires publics ou privés.

V. Bonnand, D. Pacou
(ONERA)

E-mail: vincent.bonnand@onera.fr

DOI: 10.12762/2016.AL12-04

Complex Thermo-Mechanical Approaches to Study the Behavior of High-Temperature Alloys

The work discusses the complex thermo-mechanical approaches developed at ONERA within the context of gas turbine component fatigue tests. Emphasis is placed on the general experimental methods to test nickel-based single crystal superalloys used in gas turbine blades under severe thermal and mechanical conditions. First, the successive steps required in combined thermal and mechanical fatigue testing are briefly discussed. Particular focus is placed on the techniques developed to reliably control and measure temperature fields generated by induction heating. The main experimental techniques used for thermo-mechanical testing are then discussed. Here, an axial-torsional thermo-mechanical fatigue (TMF) testing rig used to study the coupling effects of combined thermal and mechanical loads is described. How a thermal gradient is introduced in the TMF specimens to reproduce the internal air cooling technology of modern gas turbine blades is shown. In order to increase the representativeness of in-service conditions, the problem of thermo-mechanical fatigue coupled with thermal gradients is investigated using smooth, multi-perforated, and thermal barrier coated samples. It is shown that such testing capabilities can reproduce realistic thermomechanical loading conditions typical of service and constitute a powerful means to develop and validate fatigue life prediction methods. Furthermore, the effect of an overheating event that can occur during a one-engine-inoperative event during in-service operation is also investigated. This type of engine malfunction is known to lead to a degradation of the microstructure, which can modify the material constitutive behavior and affect the remaining lifetime. Finally, the additional complexities associated with the creep-fatigue interaction, the required constitutive models and the computational challenges are discussed.

Introduction

Most industrial components operating at high temperatures, such as those in gas turbines, present a complex thermal loading including high temperature, rapid temperature transient and temperature heterogeneity. The case of single-crystal turbine blades is particularly representative of the level of complexity reached in the rotating components of an aero-engine. These turbine blades are subjected to combined thermal and mechanical loading (Figure 1). They are subjected to a centrifugal force directly correlated to the rotation speed. The resulting mechanical stresses are cycled according to the operational speed of the engine. The aerodynamical loading inherent to rotative machines generates low stress amplitude at a high frequency. In parallel, these blades are the hottest components in the gas turbine. They reach heterogeneous temperatures above 1100°C. Moreover, in order to avoid failure resulting from excessive operating

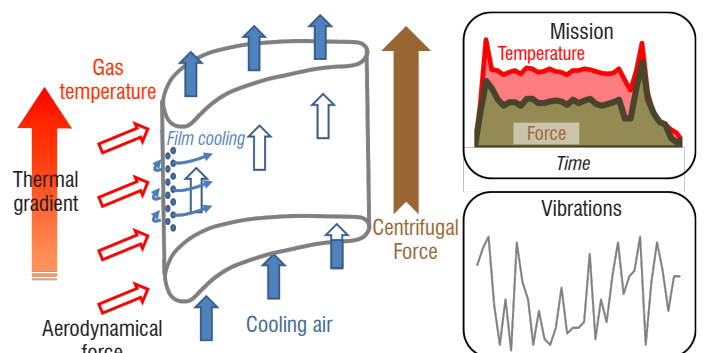


Figure 1 – Schematic description of the complex thermo-mechanical loading of turbine blades

temperatures, turbine blades often use many cooling methods, such as internal channels, film cooling and thermal barrier coatings. These cooling technologies favor temperature heterogeneity and generate thermal stresses to be superimposed on the mechanical loading.

A combined thermal and mechanical loading may develop into various damage mechanisms, such as fatigue, creep, oxidation and also microstructural evolutions. However, the significant interactions between these degradation mechanisms are quite complex, and the prediction of thermo-mechanical damage from basic properties remains difficult. There is an industrial and scientific need to generate material test data under non-isothermal service conditions. In order to be of a good quality, the tests must be conducted in the well-controlled environment of a laboratory.

Over the last six decades, non-isothermal fatigue testing has become an increasingly important method for design, material performance and reliability assessment. In the early 60's, many of the experiments involved thermal cycling. Thermal Fatigue became the terminology adopted for tests with no external mechanical loading. First, thermal fatigue test devices are essentially the same as that designed originally by Coffin [14] and later modified by Carden [10]. Here, a repeated temperature fluctuation in a restrained tube produces cyclic thermal stresses and strains, which lead to fatigue cracks. Another approach to thermal fatigue was also developed on component-like specimens, such as Glenn's tapered discs or wedge shaped specimens tested in fluidized beds [18], or rigs based on heating by the flame of a burner and cooling by compressed air [44]. In these cases, the stresses and strains obtained in the specimen are self imposed, due to the differential thermal expansion brought about by temperature gradients. An example of thermal analysis of the wedge specimens is given in [28]. At ONERA, Chaboche [11] investigated in 1972 the viscoplastic behavior of high-purity Aluminum under thermal cycling. The exploratory test specimen is presented in Figure 2. The hottest zone can reach 200°C with two infrared lamps. The cycle was based on two hold times; the longest one was at the maximal temperature of 200°C, whereas the second one was performed at 90°C.

In parallel to the thermal fatigue improvements, the necessity to perform thermomechanical experiments with externally-imposed loading appears necessary to support constitutive model developments. The

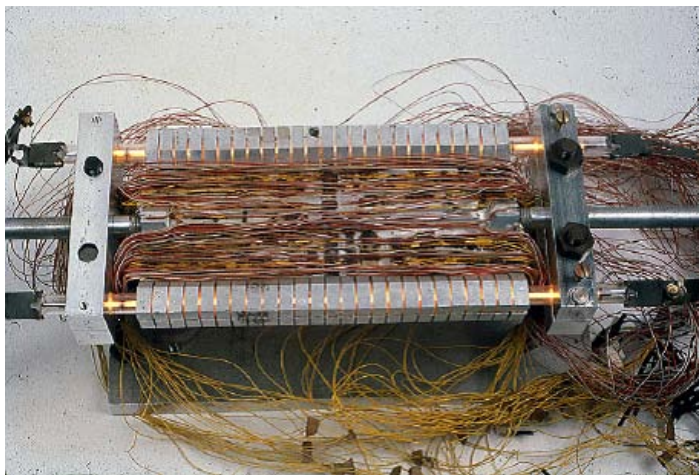


Figure 2 – Pioneering specimen equipped with 60 thermocouples and 40 strain gauges for thermal gradient fatigue (1972). The specimen is heated by two infra-red lamps inside the two external columns and cooled in the middle by a water inlet [11]

generation of precise thermomechanical response data has become possible with the development of closed-loop servohydraulic testing machines [20]. The term "thermomechanical fatigue" became dedicated to strain-controlled non-isothermal tests. Today, the literature references highly thermo-mechanical fatigue. For an overview of more recent activities in this field, the reader should refer to Remy [41], McGaw [36], and Hähner [19] in a special issue of International Journal of Fatigue. Currently, one of the challenges for the topic of thermal and mechanical fatigue is to increase the representativeness of the thermo-mechanical loading compared to the in-service conditions, as well as the representativeness of the specimen compared to real structures.

The overall objectives of the thermo-mechanical approaches discussed in this experimental research are to:

- test calculation methods to improve the life prediction,
- understand the mechanisms that govern non-isothermal damages and appear significantly different to those in the isothermal cases.

This paper reveals why non-isothermal fatigue is a more complex test technique that requires higher skills than traditional mechanical testing. The experimental approaches developed here clearly show the proximity of the turbo-engine industry. Four kinds of non-isothermal fatigue are presented, according to an industrial thermal feature of turbine blades representing the hottest parts of aircraft or helicopter engines. The first step is the characterization in pure thermo-mechanical fatigue when temperature homogeneity is considered. The second step includes a thermal gradient in the specimen wall, as encountered in cooled turbine blades due to internal cooling channels. The third topic is dedicated to severe overheating, which can be encountered in a helicopter engine. In this case, only one exotic cycle appears to be non-isothermal and plays a key role on the remaining life duration of the piece. Finally, the Thermal Barrier Coating within the context of thermal gradient mechanical fatigue will be discussed for the original thermal calibration approach developed.

Thermal aspects in thermal and mechanical testing

This section details the heating system and the temperature measurement and control methods used in the various non-isothermal testing approaches.

Heating methods

High-temperature mechanical testing requires a specific heating system suitable for a servo-hydraulic or electromechanical device. Currently used techniques include resistance heating, radiant heating and (direct or indirect) induction heating. Nevertheless, under non-isothermal conditions, the test cycle is basically based on engine flight, often combining take-off, cruising and landing in the most simplified case. In order to achieve a reasonable test duration in a laboratory, the thermal cycle is accelerated so the temperature ramp rates may exceed 10°C/s and cannot be achieved by conventional resistance furnaces.

Although radiant lamp furnaces or induction coil systems offer a high heating rate capability, another technical possibility comes from burner heating. This type of expensive device consists of a real combustion chamber. It enables the reproduction of experimental conditions close to those encountered in turbo-engines. For this purpose, a burner rig appears interesting to obtain a very high temperature testing device with high heating and cooling rates. The cooling rates can reach 60°C/s due

to the ceasing of the burning and may subject the material to quenching. The MAATRE burner developed at ENSMA – Institut Pprime illustrates the associated metrology and the performance of this test bench [38].

For complex thermo-mechanical approaches, induction heating was preferred to the radiant lamp furnace. It offers a far cheaper and more reliable solution and especially presents the high reactivity required to simulate fast cycles. Another advantage is the possibility of adapting the induction coil to a specific specimen or for measurement access. It could also be a significant drawback, because this operation is time-consuming and cannot easily offer temperature homogeneity as would be the case in a conventional radiant furnace. The different induction coils presented in this paper are always suitable for the constraints and needs of the experiments. Furthermore, the induction coil may provide the ability to perform, as far as possible, in-situ measurement techniques, such as visible image acquisition for Digital Image Correlation, or Infra-Red images for thermography.

In order to properly use induction heating, it is very important to understand the basics. The important feature of the induction heating process is that the heat is generated inside the specimen itself, instead of by an external heat source. Indeed, an inductor coil generates a variable magnetic field. If an electrical conductive part is placed inside this magnetic field, it carries the electrical current induced, also called Foucault currents. In accordance with the Joule effect, the movement of the electrons creating these currents dissipates the heat in the material. Thus, two basic parameters of this heating method must be taken into account:

- The penetration length that characterizes the distribution of the electrical current.
- The dissipated power in the specimen that characterizes the efficiency of the electrical phenomena.

For a semi-infinite plate, the penetration length p is given by the distance from the surface to a density equal to J_0 / e . It is expressed by:

$$p = \sqrt{\frac{1}{\pi f \sigma \mu}} \quad (1)$$

where σ is the electrical conductivity of the material, μ the magnetic permeability, and f is the frequency of the alternative magnetic field.

The electrical current distribution in the specimen depends on the frequency of the induction unit. Our set-ups are based on a middle-frequency unit at 100 kHz. Few data are available on the electrical resistivity of a Ni-based superalloy. By considering the superalloy CMSX-4 [40], the penetration length is estimated to be 0.72 mm at 1000°C, compared to our specimen thicknesses (1 or 2 mm).

Temperature measurement and control

In high-temperature mechanical testing, the various temperature measurement methods, which can be used either separately or in combination, are:

- thermocouples (N or S type),
- pyrometer,
- infrared camera,
- thermal paintings.

From a global point of view, spot-welded thermocouples are preferred for temperature measurement. Pyrometers and IR cameras depend

on the emissivity. Without a stable surface emissivity, results can prove to be inaccurate (temperature drift), as the specimen oxidizes and its emissivity is modified accordingly. Moreover, oxide layer cracking during a test can also significantly alter the measurement. With regard to the thermal painting, only irreversible ones are available at high temperature. This means that they cannot be used under thermal cycling within the context of a gas turbine.

Nevertheless, the presence of a spot-welded thermocouple is not acceptable in the gauge length during a fatigue test because it could cause an alteration in the material and the welded zone might be a preferential site for crack initiation. For this reason, spot-welded thermocouples are used only on specimens for calibration of the nominal temperature, according to the TMF standards [1, 5 and 25]. However, a thermocouple control can be spot-welded outside the gauge length. Indeed, all of the experiments presented in this research have additional water cooling at the specimen grips. This allows the gauge length to remain the hottest part of the specimen and it ensures a dynamically stable temperature field at the specimen ends. Another advantage of this approach is that the cooled ends may offer the possibility of testing new advanced materials that exhibit a very high temperature resistance. In ONERA's ongoing material development activities, sometimes the construction process does not allow for large specimens. This implies that the required gripping system must be machined from a lower quality alloy. Thus, a significant permanent deformation of the grips can be expected, which could also lead to their premature rupture. In return, the thermocouple is less sensitive to local temperature variations, which must be avoided by the control system.

Thermal calibration: general aspects

Calibration specimen

For non-isothermal tests, the general thermal calibration process is based on the TMF-standard [1, 25]. Before each campaign, one of the specimens is dedicated to a thermal calibration process. This step on dummy specimen is aimed at:

- optimizing the inductor coil, in terms of geometry and positioning,
- mapping the temperature field on the heated specimen.

As the basic element of a non-isothermal test, the heating system set-up (power and inductor shape) must be optimized on the calibration specimen with respect to a temperature field, which must be as uniform as possible, and to the thermal cycle. This means that thermal homogeneity must be guaranteed at each instant of the cycle. Classically, the desired zone represents at least the gauge section of the specimen. Nevertheless, it is sometimes not possible under complex thermal situations, as presented in Figure 3. Thus, another strategy

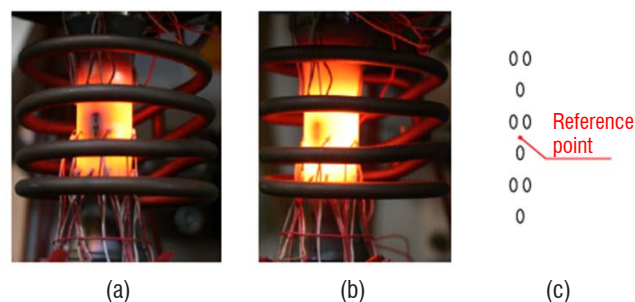


Figure 3 – Impact of the positioning of the induction coil on the temperature distribution in the case of thermal Gradient Mechanical Fatigue on a perforated specimen. (a) Initial cold area for a symmetric position (b) Minimized cold area (c) Reference point for temperature measurement by optical pyrometry

consists in measuring and controlling the nominal temperature at a reference point on the specimen. In this case, we do not seek to avoid temperature heterogeneity, but rather to measure precisely the thermal field of the outer surface. The map must be integrated analytically or numerically using a finite element approach with conventional data interpolation methods.

Whatever the strategy, based on the temperature uniformity sought or on the temperature field subjected to, thermal profiling is required based on thermal imaging or mapping by several thermocouples fixed along and around the specimen. The points of interest given by the thermocouples must be sufficiently numerous for the measured temperatures to accurately represent the thermal gradients over the external surface of the heated specimen.

Temperature control methods

In most of anisothermal fatigue problems, the temperature cycle will remain constant throughout the duration of the test. This assumes that:

- the thermal equilibrium of the load train has been reached,
- there is a dedicated temperature measurement and an associated control system,
- the repeatability and reproducibility of the thermal cycling has been checked.

The thermal equilibrium of the load train is a preliminary step before dynamic calibration. This point is very important because our devices are always equipped with water-cooled specimen grips. It should be noted that no compressed air cooling systems are added to control temperature rates. After this, one thermocouple or pyrometer can serve to perform the temperature control on the dummy specimen. With regard to the temperature control, for simple cases, the experiment could be summarized as the application of a command signal. Nevertheless, in order to ensure the temperature stability during cycling, a control-loop is preferred. Indeed, several temperature deviation sources can be encountered, such as unintended sporadic air flows, a variation of exposure to direct sunlight, or evolution of the thermal response due to an alteration of electrical properties of the material. During the temperature control step, it is necessary to check that the temperature indicated by other non-control sensors, like the thermocouple network of infrared cameras, does not vary.

A classical control-loop system can be used for temperature cycling. All of our testing setups for non-isothermal fatigue are based on a servo-hydraulic fatigue device with the MTS Test suite software. The main advantage of this global controlling system is the possibility of generating and acquiring all of the thermal and mechanical signals synchronously. Additionally, other systems, such as image acquisition or the potential drop method can also be triggered on the command or response.

Thermo-mechanical approaches for single crystal turbine blades

This section is dedicated to thermo-mechanical cycling of uncoated specimens. A schematic description of the experimental loadings is given in Figure 4. The first described setup concerns a strain-controlled thermo-mechanical fatigue test (TMF). The following topics concern the study of Thermal Gradient Mechanical Fatigue conditions (TGMF). The experimental studies have been performed on the Ni-based single crystal superalloy called AM1.

Strain-controlled Thermo-Mechanical Fatigue (TMF)

The first equipment was designed in order to simultaneously simulate thermal and mechanical loads under strain control. The main objective is to assess the accuracy of the constitutive equations under non-isothermal conditions, as well as the accuracy of life time prediction models.

The main issue of strain-controlled TMF experiments relates to the fact that the mechanical strain cycle can only be performed by controlling the total strain applied to the specimen. This means that the thermal strain in the absence of external forces has to be compensated for in an appropriate way, in order to achieve a given mechanical strain:

$$\epsilon_{mechanical} = \epsilon_{total} - \epsilon_{thermal} \quad (2)$$

Hence, special attention must be paid to the dynamic temperature measurement and control because a temperature deviation modifies the imposed mechanical strain, obviously changing the material behavior and leading to an incorrect life duration. In order to avoid

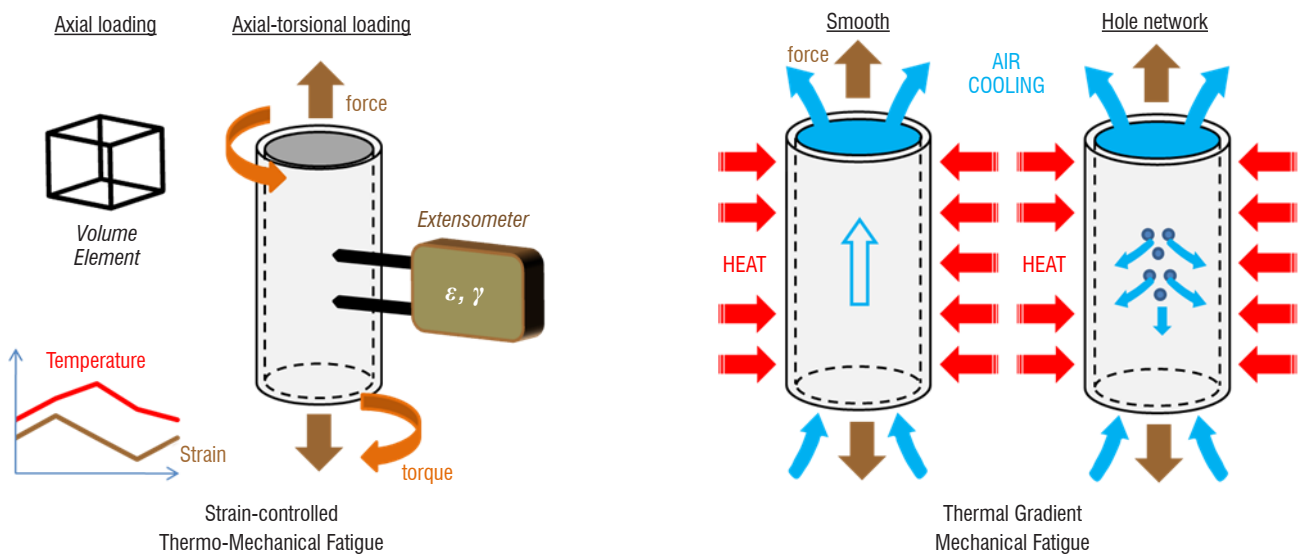


Figure 4 – Schematic description of TMF and TGMF testing developed in this research

and check it, the TMF device presented was developed according to the dedicated experimental procedure of the standard. The testing principles are detailed here ([25] and references therein) and can be divided into three main parts:

- thermal cycling under force control to record thermal strain,
- null force verification in thermal strain control,
- application of additional mechanical strain under extensometer control.

In a time-based control mode, a temperature error automatically leads to an error in the mechanical strain, according to Equation 2. This implies that special attention must be paid to avoiding temperature deviations. The second step of TMF procedure enables the stability and the reproducibility of the thermal loading to be validated. If the nominal temperature deviates or the longitudinal temperature gradient evolves, the resulting force of a thermal strain control will vary. A typical example of the thermal compensation obtained with a temperature range of 650°C to 1100°C is presented in Figure 5, also illustrating the testing rig.

Furthermore, although uniaxial thermo-mechanical fatigue is highly

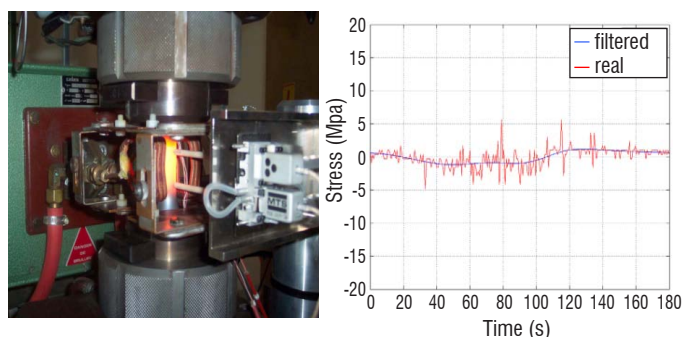


Figure 5 – Presentation of the axial-torsional TMF test device and of an axial thermal compensation cycle [7]

referenced in the literature and recently dedicated standards have appeared [1, 25], its extension to multiaxial loading remains infrequent. Axial-torsional configurations [26, 47, 7 and 9] can be discussed and, more recently, biaxial planar configurations [30, 42]. In our case, an axial-torsional loading was initially developed in [7]. Torsional loading presents specificities linked to single crystal anisotropy. On the one hand, no thermal compensation is necessary due to cubic symmetry of the thermal expansion coefficient and, on the other hand, crystalline viscoplasticity generates high strain bands in the $\langle 011 \rangle$ secondary directions. This point implies that care must be taken with the secondary direction of the crystal, in which one extensometer measures and imposes the shear strain used in the servo-loop.

It is worth noting that a comparison between tests and constitutive models could be performed based on the mechanical strain, by subtracting the thermal strain recorded during the first step from the total measured strain. An intermediate step prior to the TMF test can be introduced, in order to assess the Young and the shear moduli. The best practice consists in superimposing a force loading in the elastic regime (or, alternatively, a torque) to the same temperature cycle, as applied in the subsequent TMF test. The elastic moduli are determined as a function of temperature and then the data analysis can be done with the viscoplastic part of the strain (i.e., without the thermal and elastic strains). This research was performed using several strain-temperature paths. The experimental results have been

compared with Finite Element simulation based on crystal viscoplasticity identified for AM1. Very good agreement is observed with a temperature range between 650°C and 1100°C, as presented in Figure 6. The selected formalism including octahedral and cubic slip systems has been validated under anisothermal and multiaxial conditions [7].

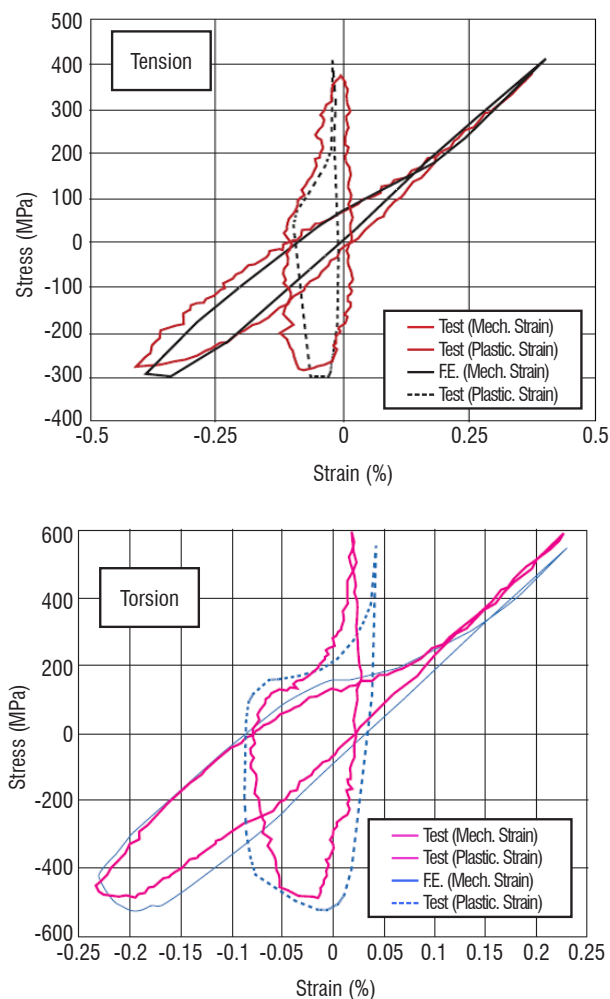


Figure 6 – Typical results for axial and torsional responses of the material [7]

Thermal Gradient Mechanical Fatigue (TGMF)

Another research topic for design engineering relates to the impact of an internal cooling system on the turbine blade life. Although anisothermal experiments are generally performed on volume elements simultaneously subjected to a controlled load and temperature, as previously presented, these tests may not be representative of cooled turbine blades, where a thermal gradient is generated over a very thin wall. The thermal strains and stresses induced by the spatial gradient during heating and cooling may be a significant cause of failure in current single-crystal blades of aero gas turbines.

In order to study the influence of the thermal gradient on fatigue life, experimental initiatives have been promoted for turbine blade analysis. At ONERA, a first experimental setup was developed at the end of the 90's [27], enabling a specific thermal gradient in the region just outside the holes of the thick specimen to be reproduced in the laboratory. Recently, this device was considerably modified and improved by [16] for thin specimens. It can be noticed that similar TGMF testing

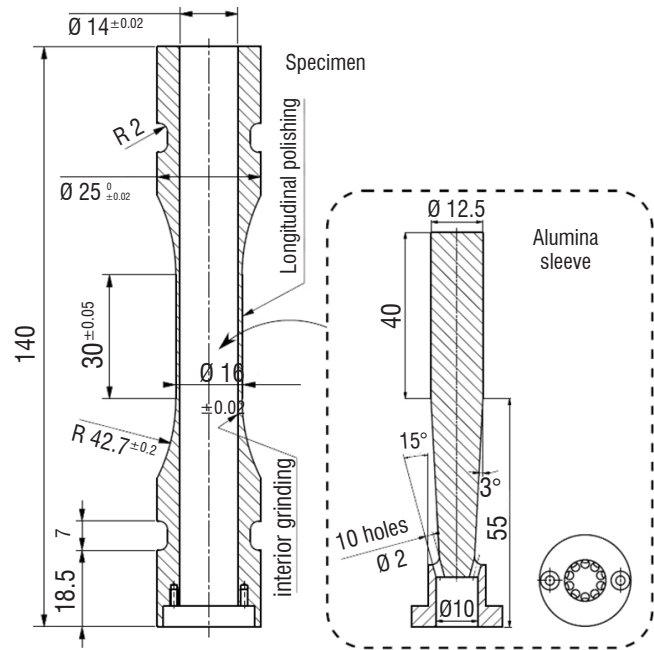
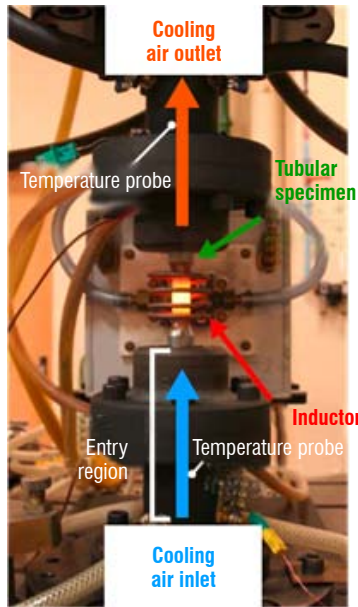


Figure 7 – Photo of the TGMF device and schema of the tubular hollow specimen with alumina sleeve

devices are still rare in the literature [13, 4, 3, 21 and 22]. Although the TGMF facility was firstly concerned with smooth specimens, their use in the presence of multi-perforations, such as on turbine blades, appears to be useful for the gas turbine industry.

TGMF on a smooth specimen

In order to simulate the temperature gradient acting on the blade, the experimental facility developed enables the cooling of the wall of the hollow cylindrical fatigue specimen, during the heating of the external wall. The difficulty lies in obtaining the highest possible thermal gradient, but with an acceptable gauge section temperature distribution. Figure 7 shows the experimental setup and the geometries of the specimen and the sleeve required to increase the heat exchange. The principle is the following one: the tubular specimen is heated by induction and a significant cold air flow is injected inside, in order to obtain a sufficient wall thermal gradient. In order to increase the air flow, and to thereby increase the thermal gradient, an alumina sleeve can be inserted into the hollow specimen.

The TGMF is characterized by (i) force-control fatigue testing, (ii) a temperature control at the external surface of the tubular specimen similar to those encountered in TMF testing, (iii) cooling of the air flow control and (iv) temperature assessment at the internal surface, characterizing the thermal gradient.

Cooling is provided by a compressed air circuit with a thermal mass flow meter at the inlet of the specimen for measuring and controlling mass flow. The mass flow meter has a maximal capacity of 53.88 g/s and a Proportional-Integral-Derivative (PID) controller. The air temperature at the inlet is 15°C and the maximal air flow reached with this installation and a mounted specimen is 43 g/s at 5 bars (28 g/s with the sleeve). The air pressure downstream from the specimen is atmospheric pressure. It is important to mention that small variations of less than 0.5 g/s around the set point are observed.

The main difficulty of this thermo-mechanical test is that the internal surface temperature cannot be measured by common methods like

thermocouples or pyrometers. In order to compensate for this lack, special attention was paid to numerically assessing the temperature gradient. The thermal problem is solved by a weak coupling between fluid and solid solvers, based on two software applications developed at ONERA, respectively Cedre and ZéBuLoN. Figure 8 presents the calculated thermal field of the specimen with the sleeve and the exchange coefficient. It exhibits a peak near the injector because the air flow is projected on to the specimen surface. This effect decreases along the specimen z axis, but an injector effect still remains up to the sleeve end. After the peak due to the injector, the exchange coefficient decreases along the specimen axis. Along the gauge length the average value is around 1100 W.m⁻².K⁻¹, which gives an average thermal gradient of 42°C.

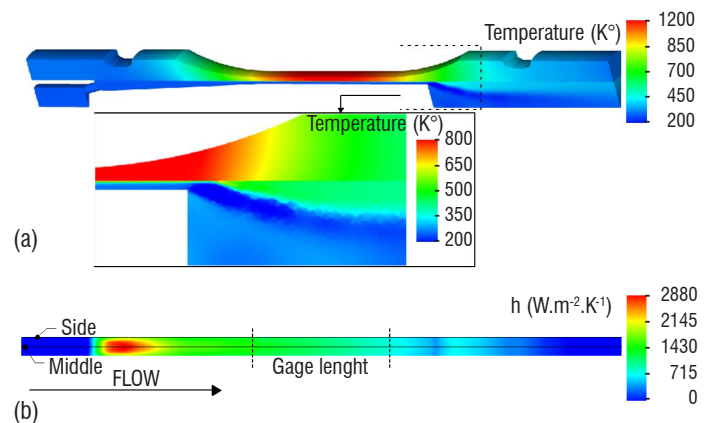


Figure 8 – Coupled calculation results (a) Specimen and air temperature fields (b) Exchange coefficient h at the interface

In order to be able to trust this internal temperature assessment numerical approach, the global heat exchange can be compared with calculations. Its evaluation is characterized by two temperature probes set upstream and downstream from the specimen. Details of the turbulent model and the resulting quite good correlation are presented in [16]. Nevertheless, improvements should be made to several calculation hypotheses, such as the adiabatic sleeve or the internal temperature distribution in the anchors.

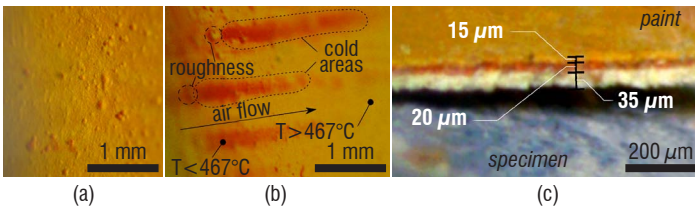


Figure 9 – Thermal paint on the internal surface after a TGMF test

An opportunity to increase the thermal gradient involves the application of thermal paint on the inner surface of the specimen. Initially added to measure the internal temperature without a thermal cycle, the thermal paint exhibited significant roughness, considerably increasing the turbulence of the cooling air flow. Figure 9 shows the roughness and gives an example of the colour gradient obtained for a thermal gradient up to 120°C/mm in the superalloy. Temperature heterogeneity is observed only close to the air injection, and the temperature gradient in the paint thickness can be also analyzed.

Afterwards, the effect of induction heating on the thermal gradient was also investigated. Induction heating allows a very high heating power and also a great responsiveness for temperature cycles. However, it has the disadvantage of heating the material itself by Joule effect, which affects wall temperature distributions. This could be calculated by considering the tube wall as a semi-infinite plate in which an analytical solution exists:

$$\dot{q}_{induction}(r) = \frac{J_0^2}{2\sigma_e} \exp\left(-\frac{2(r-r_e)}{p}\right) \quad (3)$$

where $\dot{q}_{induction}$ is the heat source generation power, J_0 is the surface current density, σ_e is the electrical conductivity, r_e is the external specimen radius and p is the penetration depth. The temperature distribution with induction heating or with surface heating (representative of radiant heating for example) can be calculated using the thermal conduction FEM. A convection coefficient h is imposed on the internal surface, associated with an air temperature $T_{air} = 15^\circ\text{C}$, as the surface temperature is T_{surf} . The thermal flux leaving the specimen is given by $q_{cool} = h \cdot (T_{surf} - T_{air})$. The surface heating is imposed through a thermal flux on the external temperature and the induction heating by thermal sources in the wall thickness. A schematic comparison of the two cases is shown in Figure 10. The temperature distribution is almost linear for surface heating, whereas it is parabolic for induction heating. The reason is that the heating power is maximal on the external surface and decreases as the distance to the internal surface decreases. It also means that for a same internal convection coefficient, the thermal gradient obtained with an induction heating system is lower than that obtained with a surface heating. The ratio ΔT between the surface heating to induction heating is virtually constant at around 1.27. This illustrates the main disadvantage of the induction heating technology.

Although the presence of a thermal gradient during pure mechanical fatigue can be investigated, a simplified engine-like cycle (Figure 11) was also defined to validate constitutive damage models in the case of realistic and complex thermo-mechanical loadings. The imposed stress cycle is in-phase with the temperature cycle. The thermo-mechanical cycle was obviously shortened to limit the test duration and to present high heat and cooling rates (65°C/s). These rates can be reached due to the high internal cooling flow. Likewise, a high power induction system is required (16 kW). During the thermal

calibration, its reproducibility was investigated according to the fluctuations of the controlled air flow. Standard deviations at the extreme values of each sub-cycle are acceptable, as illustrated in Figure 11.

Any experimental and numerical works allowed us to validate the lifetime prediction methods of the single crystal AM1. The lifetime prediction chain is obtained after solving the thermal problem. The stresses and strains are computed using constitutive equations. This is followed in the stabilized cycle by the calculation of the lifetime prediction itself, which is the determination of the number of cycles for crack initiation. Fully reversed cycles at 950°C and complex thermo-mechanical cycles have been investigated. The life prediction chain was confronted with experimental measurements in terms of mechanical response, damage localisation and crack initiation lifetime. The results are detailed in [16]. It is worth noting that necking

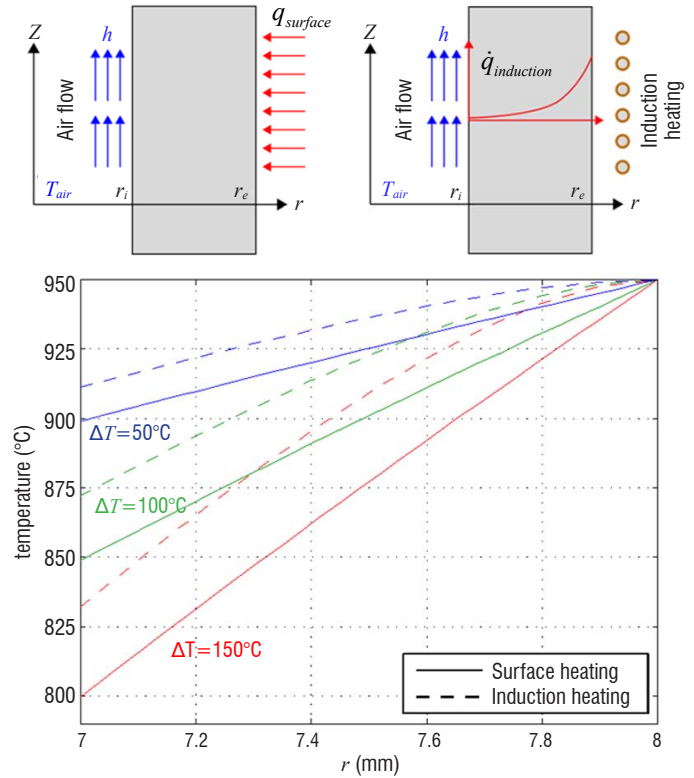


Figure 10 – Comparison of the calculated thermal gradient between the induction and the surface heating for various exchange coefficients and an external surface temperature of 950°C

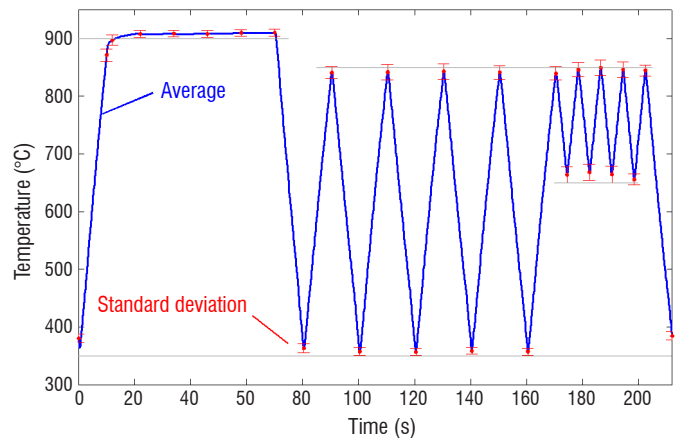


Figure 11 – Engine-like external surface temperature measured on a specimen over 30 cycles

phenomena occurred for high stress levels leading to a lower number of cycles for crack initiation than those simulated. For future works, this leads us to pursue TGMF tests under the strain control mode.

TGMF on a perforated specimen

In civil or military applications, the geometry of air-cooled blades becomes very complex, with areas involving a cooling hole-pattern at the leading edge of turbine blades. These geometrical singularities where cracks can initiate induce significant mechanical gradients additionally to the thermal one. The experimental device previously presented allowed us to evaluate the influence of these multi-perforations on the local behavior and life time.

The drilling pattern representative of areal blade was adapted for a tubular specimen with 8 mm radius; the channels are tilted with a 400 μm diameter.

In this research [16], a constant thermal gradient with fatigue cycle and engine-like cycle are also performed. Once again, a numerical analysis was performed in order to adequately compute the thermal fields inside the cooling channels. The same approach was carried out with coupled calculations in Thermal Solid/Fluid mechanics [29]. Here, the temperature control at the outer surface was performed by a pyrometer pointing at the reference point discussed in Figure 3. In order to compensate for the heat sinks represented by the holes, the inductor coil was off-centre, the injected power being dependant on the distance between the surface

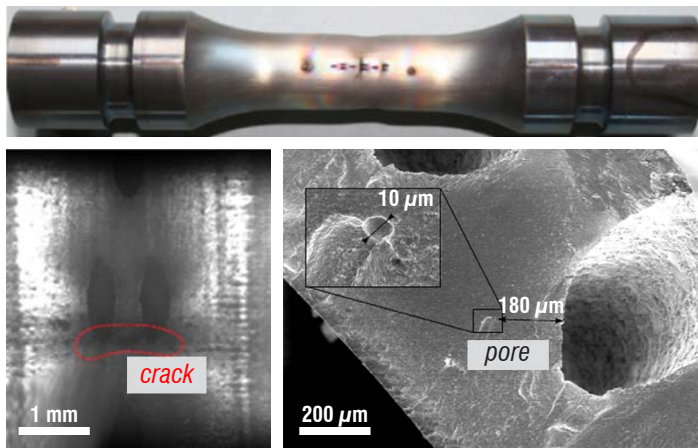


Figure 12 – Optical and SEM observations with localized necking and crack initiation linked to the interaction between holes (from [16])

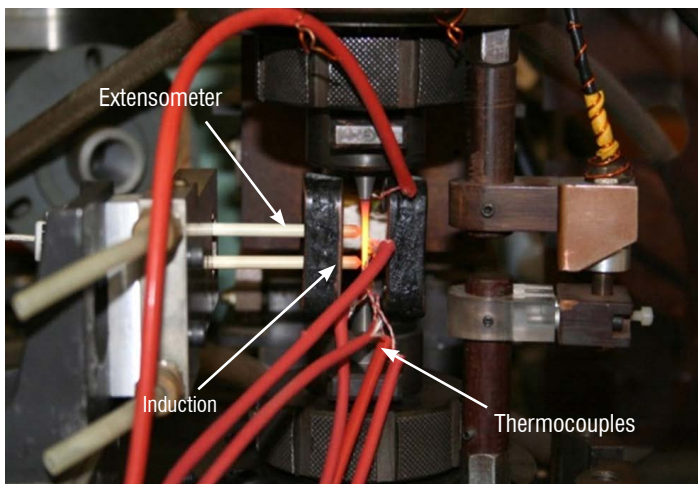


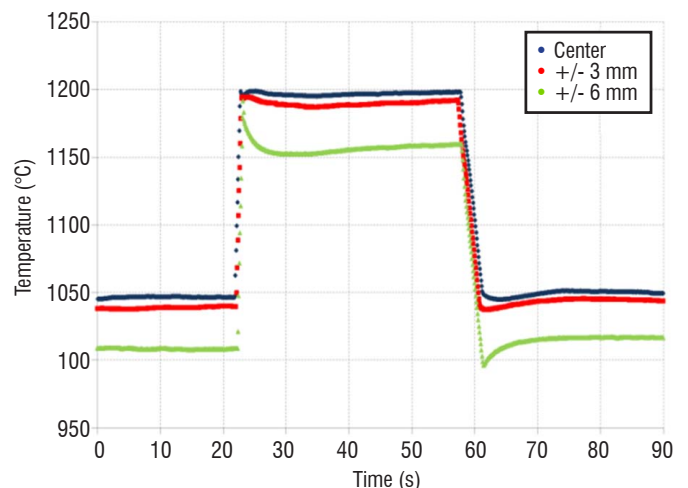
Figure 13 – Presentation of the OEI fatigue test device with induction coils and the thermal response during the OEI event (from [33])

and the coil. Nevertheless, a strong necking is always localized near a two-hole row up to the opposite side of the specimen, as observed in Figure 12. The measured circumferential thermal gradient (100°C) seems to generate a high level of creep in the hottest area. For the two tests performed at different stress range, cracks are nucleated in the two-hole row of the middle pattern. Nevertheless, it appears difficult to know the precursory mechanism between necking and crack initiation. A future investigation using digital image correlation may provide some answers.

The experimental simulation of the One-Engine-Inoperative event in turbine blades (OEI)

Although thermomechanical cycling is representative of the classically localized conditions experienced by components during the take-off, cruising, descent, and landing cycle of an engine, the rare and sudden appearance of an engine failure must also be explored. Indeed, during in-service operation of twin-engine helicopters, one of the two engines may unexpectedly be cut off. This implies a sudden temperature rise, up to 1200°C in some sections of the high pressure turbine blades for the remaining operating engine. This kind of event is called a One-Engine-Inoperative (OEI) rating, and is now included in helicopter turbo-engine certification procedures [15]. Consequently, fatigue-creep tests under isothermal conditions became insufficient to tackle the characterization of mechanical properties under non-isothermal loading conditions.

Here, the main challenge consists in reproducing this sudden temperature increase in the laboratory, by avoiding any temperature overshoot (Figure 13). In order to achieve this goal, a special inductor was required (i) to enable accessibility for an extensometer (ii) to allow good temperature homogeneity and (iii) to offer the good electrical efficiency needed for a high heating rate. The longitudinal gradient and its evolution during the OEI indicate that the gauge length is essentially heated by conduction. Indeed, the volumetric heat source distribution representing the induction heating is more localized outside of the gauge length, leading to a small overshoot outside of the gauge length. This is not an inconvenience due to the lower temperature. We can specify that this thermal response can be obtained only with temperature-loop control (Proportional-Integral-Derivative controller). Indeed, the microstructural evolution seems to significantly alter the electro-magnetic properties of the superalloy, modifying the thermal response. This special handling of the temperature control enables us to achieve temperature levels and heating/cooling rates like those encountered in a real OEI event.



The influence of an OEI event on mechanical responses has been well studied under creep conditions [34] and also in cyclic loadings [32]. The study of the creep-fatigue tests for $\langle 001 \rangle$ and $\langle 111 \rangle$ oriented specimens has shown that the plastic strain rate always decreases after one overheating. The results obtained provide some information on the effects of fine γ' precipitates on the mechanical behavior (Figure 14) and emphasize the kinetics of precipitation and dissolution, as detailed in [31, 33]. These tests revealing a strong crystallographic orientation effect on the anisothermal conditions are also extended in a multiaxial configuration (axial-torsional) [35]. Finite element simulations using a crystal-plasticity microstructure-sensitive model are necessary to understand the intricate experimental stress redistribution caused by the anisotropy of the material and are discussed elsewhere [15].

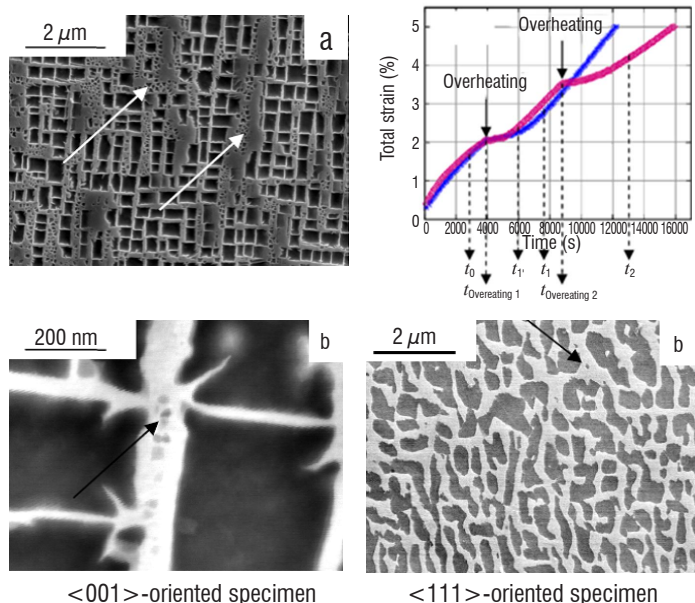


Figure 14 – Microstructures observed after overheating for 180s, with arrows indicating a γ channel with fine precipitates (from [33]) – On the left: general view and blown-up focusing on the $\langle 001 \rangle$ specimen; on the right: Plastic strain evolution during creep-fatigue experiments and the associated microstructure for the $\langle 111 \rangle$ specimen

The peculiar case of thermal barrier coating

As a next step after the internal cooling system applied to turbine blades, Thermal Barrier Coatings (TBC) are often used on the turbine blades to decrease the service temperature down to over 100 °C. TBC are a multilayer system including a thermal insulating porous ceramic layer, mostly of 8 wt.% yttria partially stabilized zirconia, deposited on an alumina-forming metallic bond coat in contact with the single crystal superalloy substrate.

In service, the structure and composition of each layer can evolve, due to sintering of the ceramic layer, oxidation of the bond coat, and inter-diffusion phenomena with the substrate. This affects the mechanical properties, such as the interfacial toughness, and consequently may cause the ceramic layer to spall off in the end. For more details on these degradation mechanisms, the reader is referred to [2]. For industrial partners, the lifetime assessment of TBC systems has been a challenge and a goal of prime importance since their introduction in aircraft engines. For this purpose, an energetic based model was developed at ONERA and calibrated by means of adhesion tests [43,45, 24, 12].

It is well known that, in the presence of a sufficiently large thermal gradient, cracks form and propagate on delamination planes in the TBC parallel to the interface, resulting in regions that spall away, leaving a thin layer of zirconia still attached to the substrate [23]. In the literature, experimental studies are often limited to thermal cycling without external mechanical loading [41,39], even if the degradation mode does not arise either when the system is thermally cycled within a furnace or when tested in a burner rig. In order to fill such a gap, the TGMF device previously presented was adapted for Thermal Barrier Coatings. The set-up evolution results from the knowledge of the thermo-physical properties of yttria partially stabilized zirconia. We decided to take advantage of its significant ionic conductivity at high temperatures [17]. This enables us to pursue the heating of a coated specimen by the induction system. From room temperature, only the substrate will heat by the Joule effect induced by the magnetic field and, given that the specimen temperature will increase, a consistent part of the heat will be directly generated in the TBC. In order to evaluate the temperature gradient in the wall thickness of a tubular specimen, thermal computations are performed with the following considerations:

- forced internal convection (exchange coefficient h provided by coupled aerothermal/solid simulation in the case of an uncoated specimen [16]),
- Joule effect in the superalloy (exponential curve of the heat source, linked to induction),
- Joule effect in the TBC (significant ionic conductivity in the TBC at high temperatures [17]),
- natural external convection.

Figure 15 clearly shows that, at a high temperature, ionic conductivity enables an adequate thermal gradient to be obtained in the coating, particularly when tests are performed with a sleeve. The temperature appears to be quite constant across the TBC, compared to the hypothetical case of a non-conductive coating.

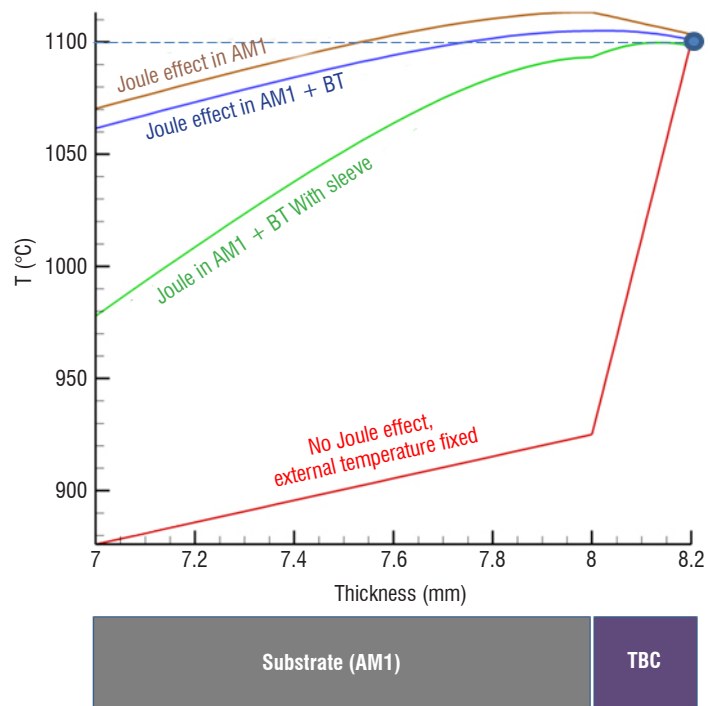


Figure 15 – Estimated thermal gradient in the coated specimen thickness, according to several assumptions regarding the heat generation for an external temperature of 1100°C

The temperature at the metal/oxide interface is well known to be a key parameter for the system lifetime assessment. Nevertheless, this interface temperature is not easily accessible by conventional measurement methods. Moreover, a thermocouple cannot obviously be welded on to the TBC due to its nature. Although Manara *et al.* [37] measured the optical properties of this semi-transparent medium, the real emissivity of the coating and its evolution remains unknown. In order to evaluate the interface temperature precisely during thermal cycling, an original thermal calibration procedure was proposed by a coupled experiment/calculation approach. On a dedicated specimen, an artificial spallation was made manually. The specimen is then meshed with the coating including the spalled zone. A set of thermal calculations enable us to obtain the relationship between the temperatures at different locations. First, the calibration test enables the temperature pointed by pyrometer at the thermal barrier coating and that measured by a thermocouple spot-welded in a spalled superalloy to be linked. For a fixed emissivity parameter, this link is a function of the internal cooling and of the external temperature. The numerical simulations offer the relationship between the exposed substrate and the interface temperature far from the spallation. Afterwards, a heating power chart can be achieved to assess the interface temperature.

Another challenging point is the determination of the service life of the thermal barrier; it is crucial to be able to distinguish the first steps of the TBC spallation. A simple way is to take advantage of the contrast of optical images, which is linked to the emissivity variation between the TBC and the natural oxide layer. Optical mirrors are added, in order to observe the entire circumference of the hollow specimen. Figure 16 shows an example of the spallation observed at a high temperature (1100°C).

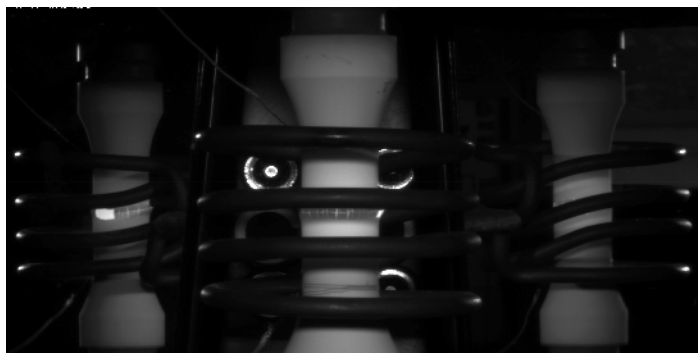


Figure 16 – Examples of the image captured at a high temperature (Observation in one shot of significant spallation in the left mirror)

First, preliminary tests are performed to validate the ability of the TGMF testing device for a coated specimen. The thermal cycles in their experiments consisted of a 60 minute exposure to a temperature of 1100°C at the interface between the TBC and the superalloy, followed by a 2 min air cooling prior to a 2 min reheating. The thermal gradient over the wall thickness introduces another source of complexity. In future studies, this device will allow us to analyze the degradation mechanisms of TBC under representative thermal gradient conditions. Obviously, a simulated thermal map deduced from experiments should be transferred into 3D Finite Element simulations, in order to perform lifetime calculations, which should be compared with lifetime assessment tools for thermal barrier systems.

Conclusions & Perspectives

The strong demand from aero-engine manufacturers and certification authorities to improve the fatigue life assessment of gas turbine blades has led to the development of advanced thermo-mechanical fatigue testing. ONERA's activities in this field have traditionally been associated with the prediction of the complex associated phenomena. These specific experimental developments have been performed to underpin the development of lifeing methods and/or to gain a greater understanding of fatigue behavior and its associated mechanisms under realistic anisothermal conditions. The present work has focussed on the thermo-mechanical approaches developed at ONERA to study successively the superposition of thermal and mechanical loadings, the impact of a thermal gradient and of turbine blade overheating during a one-engine-inoperative event, and coated test specimen behavior under thermal gradient mechanical fatigue. A common feature of these complex experiments is that advanced numerical studies are required to analyze the effect of complex service thermal loading at either the component and/or the microstructure level.

It has been shown that axial-torsional thermo-mechanical fatigue testing enables the validation of the superalloy behavior under anisothermal conditions. Moreover, it is known that the cooling systems in gas turbine blades enhance the role of high temperature fatigue when compared to uncooled blades, where creep is dominant. The presence of holes on cooled blades also affects the component lifetime, and such behavior must be taken into account by life prediction methods. Models also need to be validated against the combined effects of temperature and stress gradients and, in some cases, thermal barrier coatings under these realistic conditions. Finally, an investigation into the implications of turbine malfunction, such as the one-engine-inoperative event required by certification authorities, regarding the microstructural degradation and associated changes in high-temperature material behavior has enabled ONERA to adapt fatigue life models accordingly.

The representativeness of in-service loading conditions for the fatigue testing of gas turbine materials is always an experimental challenge. In the future, these complex tests will continue to be strongly underpinned by computational models. Future studies will be more driven to account for the ever-increasing complexity of thermo-mechanical loading conditions, which need to be reproduced at the laboratory scale. For instance, accumulative anisothermal fatigue with high cycle fatigue, like multiaxiality [8], will need to be properly evaluated when designing and predicting the life of engineering components. Furthermore, the extension of these complex thermo-mechanical approaches to incorporate crack growth is still in its infancy. By developing effective fatigue testing facilities and by enriching existing measurement methods with advanced imaging, thermography, and tomography techniques, etc., it is expected that the fatigue durability assessment of gas turbine engine components will become increasingly realistic in the future ■

Acknowledgments

These works are also the fruit of trainee and doctoral students. The authors wish to sincerely thank J. B. Le Graverend (currently at Texas A&M University, USA) for the OEI testing and analyzes, R. Degeilh (currently at EDF Lab Saclay, France) for the development of the TGMF device and J. C. Anglès (currently at Stanford University, USA) for the TBC study. The authors would like to thank J. D. Garaud and ANDHEO for their precious help in performing the coupled simulations. Furthermore, the authors are also particularly grateful to the SNECMA – SAFRAN group for providing the material and to the French Ministry of Defence for its financial support. The main part of these works was conducted under the French program “PRC Structures Chaudes” involving the SNECMA-SAFRAN group, the Turbomeca-SAFRAN group, ONERA and other laboratories.

References

- [1] ASTM. E 2368-04 - *Standard Practice for Strain Controlled Thermomechanical Fatigue Testing*. Philadelphia (2004) PA, 3.01
- [2] M.-P. BACOS, J.-M. DORVAUX, O. LAVIGNE, R. MEVREL, M. POULAIN, C. RIO, M.-H. VIDAL-SETIF - *Performance and Degradation Mechanisms of Thermal Barrier Coatings for Turbine Blades: a Review of ONERA Activities*. Aerospace Lab Issue 3, 2011.
- [3] M. BARTSCH, B. BAUFELD, S. DALKILIC, L. CHERNOVA, M. HEINZELMANN - *Fatigue Cracks in a Thermal Barrier Coating System on a Superalloy in Multiaxial Thermomechanical Testing*. International Journal of Fatigue 30 (2008) 211-218.
- [4] B. BAUFELD, M. BARTSCH and M. HEINZELMANN - *Advanced Thermal Gradient Mechanical Fatigue Testing of CMSX-4 with an Oxidation Protection Coating*. International Journal of Fatigue, 30:219-225, 2008.
- [5] T. BECK, P. HAHNER, C. RAE, E. AFFELD, H. ANDERSSON, A. KOSTER, M. MARCHIONNI - *Standardization Thermo-Mechanical Fatigue – The Route to the Standardization (TMF-Standard Project)*. Materials and Corrosion, 57, N°1.
- [6] T. BECK, K. RAU - *Temperature Measurement and Control Methods in TMF Testing – A Comparison and Evaluation*. Int. Journal of Fatigue, 30, p. 226-233, 2008.
- [7] V. BONNAND - *Etude de l'endommagement d'un superalliage monocristallin en fatigue thermo-mécanique multiaxiale*. Thèse ENSMP-ONERA, 2006.
- [8] V. BONNAND, J. L. CHABOCHE, P. GOMEZ, P. KANOUTÉ, D. PACOU - *Investigation of Multiaxial Fatigue in the Context of Turboengine Disc Applications*. International Journal of Fatigue, 33-8, p. 1006-1016, 2011.
- [9] S. P. BROOKES, H.-J. KÜHN, B. SKROTZKI, H. KLINGELHÖFFER, R. SIEVERT, J. PFETZING, D. PETER, G. EGGELER - *Axial-Torsional Thermomechanical Fatigue of a Near- γ TiAl-Alloy*. Materials Science and Engineering: A, Volume 527, Issues 16-17, 25 June 2010, p. 3829-3839.
- [10] A. E. CARDEN and T. B. SLADE - *High-temperature Low-cycle Fatigue Experiments on Hastelloy X, Fatigue at High Temperature*. ASTM STP 459, 1969, p. 111-129.
- [11] J.-L. CHABOCHE - *Calcul des déformations visco-plastiques d'une structure soumise à des gradients thermiques évolutifs*. Thèse de Doctorat de 3^{ème} cycle, Orsay, 1972.
- [12] J.-L. CHABOCHE, F. FEYEL, M. POULAIN, N. RAKOTAMALALA, A. ROOS, J.-R. VAUNOIS, A. LONGUET, AND P. KANOUTE - *Lifetime Assessment Tools for Thermal Barrier Systems in "Thermal Barrier Coatings IV"*. German Aerospace Center; ECI Symposium Series, 2015.
- [13] J.-L. CHABOCHE, J. P. CULIE, F. GALLERNEAU, D. NOUAILHAS, D. PACOU AND D. POIRIER - *Thin Wall Thermal Gradient: Experimental Study F.E. Analysis and Fatigue Life Prediction*. 5th International conference on biaxial/Multiaxial Fatigue & Fracture, Cracow (Poland), 1997.
- [14] L. F. COFFIN - *A Study of the Effects of Cyclic Thermal Stresses on a Ductile Metal*. Transactions of ASME, 1954, vol. 76, p. 931-950.
- [15] J. CORMIER, F. MAUGET, J. B. LE GRAVEREND, C. MORICONI, J. MENDEZ - *Issues Related to the Constitutive Modeling of Ni-based Single Crystal Superalloys under Aeroengine Certification Conditions*. Aerospace Lab Journal vol.7, August 2015.
- [16] R. DEGEILH - *Développement expérimental et modélisation d'un essai de fatigue avec gradient thermique de paroi pour application aube de turbine monocristalline*. thèse LMT Cachan-ONERA, 2013.
- [17] J. W. FERGUS - *Electrolytes for Solid Oxide Fuel Cells*. Journal of Power Sources, Volume 162, Issue 1, 8 November 2006, p. 30-40.
- [18] E. GLENNY - *A Study of the Thermal-Fatigue Behaviour Metals*. Journal of the Institute of Metals, Paper No 2010, 1970, p. 449-461.
- [19] P. HAHNER, C. RINALDI, V. BICEGO, E. AFFELDT, T. BRENDEL, H. ANDERSSON, T. BECK, H. KLINGELHOFER, H.-J. KUHAN, A. KOSTER, M. LOVEDAY, M. MARCHIONNI, C. RAE - *Research and Development into a European Code of Practice for Strain Controlled Thermomechanical Fatigue Testing*. Int. J. Fatigue, 30 (2008), p. 372-381.
- [20] S. W. HOPKINS - *Low-Cycle Thermal Mechanical Fatigue Testing*. ASTM STP 612, 1976.
- [21] N. X. HOU, Z. X. WEN and Z. F. YUE - *Tensile and Fatigue Behavior Of Thin-Walled Cylindrical Specimens Under Temperature Gradient Condition*. Journal of Materials Science, 43:1933-1938, 2008.
- [22] N. X. HOU, Q. M. YU, Z. X. WEN, and Z. F. YUE - *Low Cycle Fatigue Behavior of Single Crystal Superalloy with Temperature Gradient*. European Journal of Mechanics - A : Solids, 29:611-618, 2010.
- [23] J. W. HUTCHINSON, A. G. EVANS - *On the Delamination of Thermal Barrier Coatings in a Thermal Gradient*. Surface and Coatings Technology 149, p. 179-184, 2002.
- [24] R. G. HUTCHINSON and J. W. HUTCHINSON - *Lifetime Assessment for Thermal Barrier Coatings: Tests for Measuring Mixed Mode Delamination Toughness*. Journal of the American Ceramic Society, 2011, 94:85-95.
- [25] ISO/FDIS 12111 - *Metallic Materials, Fatigue Testing, Strain Controlled Thermomechanical Testing Method*.
- [26] S. KALLURI, P. BONACUSE - *An Axial-Torsional Thermomechanical Fatigue Testing Technique, Multiaxial Fatigue and Deformation Techniques*. STP1280, p. 184, 1997.
- [27] P. KANOUTE, D. PACOU, D. POIRIER, F. GALLERNEAU, J.-M. CARDONA - *Thermo-Mechanical Fatigue Life Analysis on Multiperforated Components*. Temperature-Fatigue Interaction, p. 341-350, 2002.
- [28] A. KOSTER, G. LAURENT, G. CAILLETAUD and L. REMY - *Analysis of Thermal Fatigue Tests for Superalloy Components, Fatigue Under Thermal and Mechanical Loading: Mechanisms, Mechanics and Modelling*. Proc. of Symp., The Netherland, 22-24 May 1995.

- [29] S. KRUCH, P. KANOUTE, V. BONNAND - *ONERA's Multiaxial and Anisothermal Lifetime Assessment for Engine Components*. Aerospace Lab Issue 09, August 2015.
- [30] D. KULAWINSKI, A. WEIDNER, S. HENKEL, H. BIERMANN - *Isothermal and Thermo-Mechanical Fatigue Behavior of the Nickel Base Superalloy Waspaloy™ Under Uniaxial and Biaxial-Planar Loading*. International Journal of Fatigue, Volume 81, December 2015, p. 21-36.
- [31] J. B. LE GRAVEREND, J. CORMIER, F. GALLERNEAU, P. PAULMIER, *Dissolution of Fine γ' Precipitates of MC2 Ni-Based Single-Crystal Superalloy in Creep-Fatigue Regime*. Eurosuperalloy 2010.
- [32] J. B. LE GRAVEREND, J. CORMIER, F. GALLERNEAU, S. KRUCH, J. MENDEZ - *Strengthening Behavior in Non-Isothermal Monotonic and Cyclic Loading in a Ni-Based Single Crystal Superalloy*. IJF, 91 p. 257-263, 2016.
- [33] J.-B. LE GRAVEREND, J. CORMIER, M. JOUIAD, F. GALLERNEAU, P. PAULMIER, F. HAMON - *Effect of Fine γ' Precipitation on Non-Isothermal Creep and Creep-Fatigue Behaviour of Nickel Base Superalloy MC2*. Materials Science and Engineering: A, Volume 527, Issue 20, 25 July 2010, p. 5295-5302.
- [34] J.-B. LE GRAVEREND - *Étude et modélisation des effets d'incursion à très haute température sur le comportement mécanique d'un superalliage monocristallin pour aubes de turbine*. Thèse ENSMA-ONERA, 2013.
- [35] J.-B. LE GRAVEREND - *Multiaxial Thermo-Mechanical Loading at High Temperature on a Ni-based Single Crystal Superalloy*. Oral presentation @ CREEP 2015. Article in preparation.
- [36] M. A. MCGAW, S. KALLURI, J. BRESSERS, S. D. PETEVES, editors - *Thermomechanical Fatigue Behavior of Materials*. ASTM STP 1428, vol. 4. West Conshohocken, PA: ASTM International; 2002.
- [37] J. MANARA, M. AARDUINI-SCHUSTER, H.-J. RATZER-SCHEIBE, U. SCHULZ - *Infrared-Optical Properties and Heat Transfer Coefficients of Semitransparent Thermal Barrier Coatings*. Surface and Coatings Technology, Vol. 203, Issue 8, p. 1059-1068, 2009.
- [38] F. MAUGET, D. MARCHAND, G. BENOIT, M. MORISSET, D. BERTHEAU, J. CORMIER, J. MENDEZ, Z. HERVIER, E. OSTOJA-KUCZYNSKI, and C. MORICONI - *Development and Use of a New Burner Rig Facility to Mimic Service Loading Conditions of Ni-Based Single Crystal Superalloys*. Eurosuperalloys 14, 2014.
- [39] F. MAUGET, F. HAMON, M. MORISSET, J. CORMIER, F. RIALANT, J. MENDEZ - *Damage Mechanisms in an EB-PVD Thermal Barrier Coating System During TMF and TGMF Testing Conditions Under Combustion Environment*. IJF, accepted, 2016.
- [40] K. C. MILLS, Y. M. YOUSSEF, Z. LI & Y. SU - *Calculation of Thermophysical Properties of Ni-based Superalloys*. ISIJ INTER., Vol. 46, N° 5, p. 623-632, 2006.
- [41] L. REMY, J. PETIT, editors - *Temperature-fatigue interaction*. ESIS Publication 29. Amsterdam: Elsevier; 2002.
- [42] A. SCHOLZ, A. SAMIR, C. BERGER - *Biaxial Thermomechanical Fatigue Experiments with Cruciform Test Pieces*. Proc. 7th of Int. Conf. on Biaxial and Multi-axial Fatigue & Fracture, Elsevier, Berlin, p. 555-560, 2004.
- [43] J. SNIEZEWSKI, P. LOURS, Y. LE MAOULT - *Oxidation and Spallation of FeCrAl Alloys and Thermal Barrier Coatings: In Situ Investigation Under Controlled Temperature Gradient*. Materials at High Temperatures, Volume 27, Issue 2, 2010.
- [44] D. A. SPERA, F. D. CALFO and P. T. BIZON - *Thermal Fatigue of Simulated Turbine Blades*. NASA TM X-67820, National Aeronautic Space Administration, May 1971.
- [45] J.-R. VAUNOIS - *Modélisation de la durée de vie des barrières thermiques, par le développement et l'exploitation d'essais d'adhérence*. Thèse ONERA/ Université de Grenoble, 2013.
- [46] J.-R. VAUNOIS, J.-M. DORVAUX, P. KANOUTÉ, J.-L. CHABOCHE - *A New Version of a Rumpling Predictive Model in Thermal Barrier Coatings*. European Journal of Mechanics - A/Solids, Volume 42, November-December 2013, p. 402-421.
- [47] J. ZIEBS, J. MEERSMANN, H.-J. KÜHN, H. KLINGELHÖFFER - *Multiaxial Thermo-mechanical Deformation Behavior of IN 738 LC and SC 16*. IV. Symposium on Thermo-mechanical Fatigue Behavior of Materials, ASTM STP 1371, West Conshohocken, USA, 2000, p. 257-278.

Acronyms

TBC	(Thermal Barrier Coating)
TMF	(Thermo-Mechanical Fatigue)
TGMF	(Thermal Gradient Mechanical Fatigue)

AUTHORS



Vincent Bonnand received his PhD in Materials Science and Engineering from the *Ecole des Mines de Paris* in 2006. He has been working at ONERA since 2007 in the Metallic Materials and Structures Department lab. His research topics concern the experimental mechanics at the intersection of different fields, such as solid mechanics, thermal analysis, associated measurements and non-destructive technologies.



Didier Pacou has been working at ONERA as an engineer in experimental mechanics in the Metallic Materials and Structures Department, since 1978. He is in charge of the complex fatigue devices and is involved in the development of specific devices and non-destructive technologies.